Geophysical Prospecting 35, 629–655, 1987.

COMPUTATIONAL ASPECTS OF THE CHOICE OF OPERATOR AND SAMPLING INTERVAL FOR NUMERICAL DIFFERENTIATION IN LARGE-SCALE SIMULATION OF WAVE PHENOMENA*

O. HOLBERG**

ABSTRACT

HOLBERG, O. 1987, Computational Aspects of the Choice of Operator and Sampling Interval for Numerical Differentiation in Large-Scale Simulation of Wave Phenomena, Geophysical Prospecting 35, 629–655.

Conventional finite-difference operators for numerical differentiation become progressively inaccurate at higher frequencies and therefore require very fine computational grids. This problem is avoided when the derivatives are computed by multiplication in the Fourier domain. However, because matrix transpositions are involved, efficient application of this method is restricted to computational environments where the complete data volume required by each computational step can be kept in random access memory.

To circumvent these problems a generalized numerical dispersion analysis for wave equation computations is developed. Operators for spatial differentiation can then be designed by minimizing the corresponding peak relative error in group velocity within a spatial frequency band. For specified levels of maximum relative error in group velocity ranging from 0.03% to 3%, differentiators have been designed that have the largest possible bandwidth for a given operator length.

The relation between operator length and the required number of grid points per shortest wavelength, for a required accuracy, provides a useful starting point for the design of cost-effective numerical schemes. To illustrate this, different alternatives for numerical simulation of the time evolution of acoustic waves in three-dimensional inhomogeneous media are investigated. It is demonstrated that algorithms can be implemented that require fewer arithmetic and I/O operations by orders of magnitude compared to conventional second-order finite-difference schemes to yield results with a specified minimum accuracy.

* Paper read at the 47th EAEG meeting, Budapest, June 1985, final draft received December 1986.

** Formerly Department of Petroleum Technology and Applied Geophysics, The Norwegian Institute of Technology. Present address: A/S Informasjonskontroll, P.O. Box 265, 1371 Asker, Norway.

INTRODUCTION

Numerical solution of partial differential equations via finite-difference and related techniques has established itself as a valuable tool in the simulation of physical phenomena. In numerical modelling of wave propagation, such techniques yield accurate synthetic seismograms for arbitrarily inhomogeneous media. These modelling techniques may be used in more or less automated inversion procedures by perturbation of the parameters characterizing the geological medium until the synthesized records fit the observed real data.

The introduction of vector computers like the Cray X-MP has at least made three-dimensional (3-D) wave equation computations a practical reality. However, without more powerful computational systems and/or more efficient numerical methods, iterative procedures involving large-scale 3-D wave equation computations are not feasible on a routine basis.

The shortcomings of conventional methods for numerical simulation are related directly to the techniques used for numerical differentiation. Only two techniques for numerical differentiation have gained ground in numerical analysis: the classical finite-difference (FD) technique and the Fourier (pseudospectral) technique.

The conventional FD operators become progressively inaccurate at higher frequencies. Therefore, for reliable results, the ordinary FD technique requires very fine computational grids. For FD modelling of realistic seismic phenomena, a spatial sampling rate of more than 20 points per shortest wavelength is needed. In 3-D modelling, this requirement produces a huge amount of data that must be stored and retrieved for each computational step. Small-scale implementations of FD schemes for wave equation modelling are described by Kelly, Ward, Treitel and Alford (1976) and the accuracy of such schemes has been analysed by Alford, Kelly and Boore (1974) and by Marfurt (1984).

Derivatives computed by multiplication in the Fourier domain (Kreiss and Oliger 1972, Gazdag 1973, Orzag 1980) are, at least in principle, accurate to machine precision within the band that can be uniquely represented by the computational mesh. Therefore, only two grid points per shortest wavelength are required. However, this technique requires matrix transpositions for each computational step. Efficient application of the Fourier technique is therefore restricted to computational environments where the complete data volume required by each computational step can be kept in random access memory. Seismic forward modelling by the Fourier method has been described by Gazdag (1981), Kosloff and Baysal (1982), Kosloff, Reshef and Loewenthal (1984) and by Johnson (1984).

The Fourier technique corresponds to using a long convolutional operator for numerical differentiation. Clearly, one has the freedom to design operators that bridge the gap between the two extremes: the short FD operators and the Fourier technique. An empirical study of the application of high-order differencing to the acoustic wave equation for constant density has been given by Dablain (1986).

This work investigates, mainly from a computational point of view, what can be gained by using optimized convolutional operators for spatial differentiation in wave equation computations. Firstly a general link between the error in numerical

differentiation and the resultant undesired effects on the output of wave equation modelling is established. This link enables us to design optimum differentiators to control those undesired effects. The computational implications are then discussed. Different schemes for acoustic time evolution modelling are analysed to illustrate this discussion.

Review of Numerically Induced Dispersion in Wave Equation Computations

The frequency response of an operator for spatial differentiation can be written

$$D_{x_j}(k_j) = ik_j(1 + \varepsilon_j(k_j)), \tag{1}$$

where k_j denotes spatial frequency or wavenumber in the x_j direction and $\varepsilon_j(k_j)$ is the relative error in the frequency response of the differentiator.

Assume that the operator (1) is used for spatial differentiation in 3-D wave equation computations and that the error in time differentiation is neglible. In time evolution applications this can be obtained by using a small temporal sampling interval and/or by using a high-order scheme for time integration. For a homogeneous isotropic elastic medium with no damping, the dispersion relation is (see appendix A)

$$\omega^2/c^2 = \sum_{j=1}^{3} k_j^2(1 + \varepsilon_j)^2, \tag{2}$$

with

$$\varepsilon_j = \varepsilon_j(k_j),$$

where c is the physical velocity of propagation determined by the elastic parameters of the medium and ω is the temporal frequency. The phase velocity is

$$\begin{aligned} c_{\text{ph}} &= \omega(k_1, k_2, k_3)/(k_1^2 + k_2^2 + k_3^2)^{1/2} \\ &\approx c\left[1 + \sum_{j=1}^{3} (k_j/k)^2\varepsilon_j\right], \end{aligned} \tag{3}$$

with

$$k = (k_1^2 + k_2^2 + k_3^2)^{1/2},$$

when terms of higher order in ε are neglected.

If now

$$-E < \varepsilon_j < E \qquad j = 1, 2, 3 \tag{4a}$$

then

$$c(1 - E) < c_{\text{ph}} < c(1 + E) \tag{4b}$$

for all possible directions of propagation. The relative error in phase velocity is bounded by the relative error in the frequency response of the differentiator.

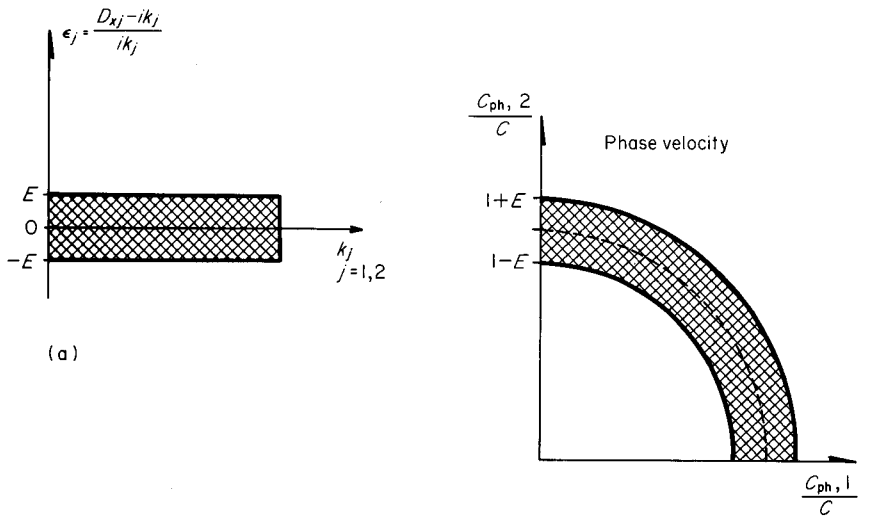

Fig. 1a. Error region for the spatial differentiators and corresponding error region for the numerical phase velocity.

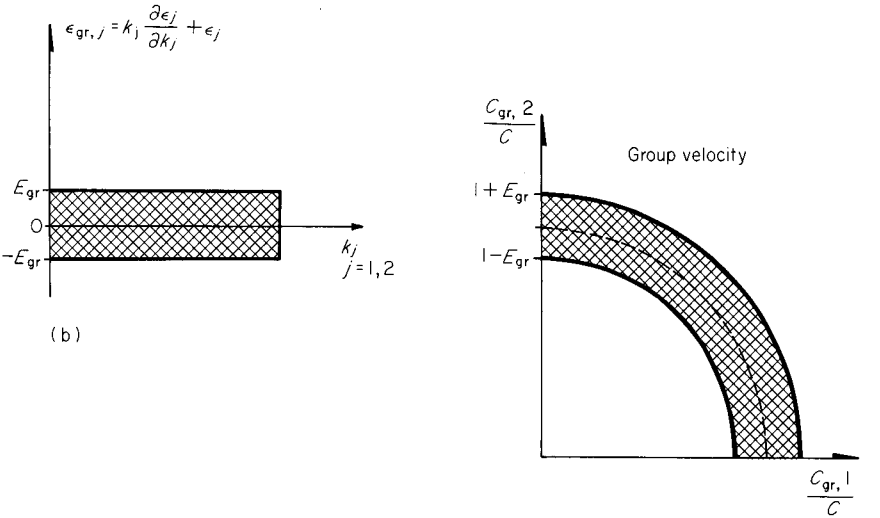

Fig. 1b. Error region for the spatial differentiators and corresponding error region for the numerical group velocity.

The propagation of energy is governed by the group velocity (Trefethen 1982). Wavenumber-dependent group velocity causes different spectral components to travel at different speeds and in the wrong directions, thereby giving rise to numerically induced dispersion, to numerical anisotropy, and, for inhomogeneous media, to frequency-dependent errors in reflection and transmission. The components of

the vectorial group velocity may be expressed as

$$\partial\omega/\partial k_j \approx (ck_j/k)\left[1 + k_j\,\partial\varepsilon_j/\partial k_j + 2\varepsilon_j - \sum_{l=1}^{3}(k_l/k)^2\varepsilon_l\right] \qquad j = 1, 2, 3 \tag{5}$$

when terms of higher order in ε and its derivatives with respect to the spatial frequencies are neglected. The absolute value of the group velocity is then

$$c_{gr} \approx c\left[1 + \sum_{j=1}^{3}(k_j/k)^2(k_j\,\partial\varepsilon_j/\partial k_j + \varepsilon_j)\right]. \tag{6}$$

The relative error in group velocity is controlled by the 1-D expressions

$$\varepsilon_{gr,j} = k_j\,\partial\varepsilon_j/\partial k_j + \varepsilon_j \qquad j = 1, 2, 3. \tag{7}$$

If

$$-E_{gr} < \varepsilon_{gr,j} < E_{gr} \qquad j = 1, 2, 3 \tag{8a}$$

then

$$c(1 - E_{gr}) < c_{gr} < c(1 + E_{gr}) \tag{8b}$$

for all possible directions of propagation. The results given by (4) and (8) are illustrated for two dimensions in figs 1a and 1b respectively.

Equations (7) and (8) set error bounds to the absolute value of the group velocity vector. From (5) it is seen that the relative error in the components of the group velocity vector, and hence the directional errors, are bounded when both the relative group errors defined by (7) and the phase errors are bounded. More precisely, if (4a) and (8a) both hold, then

$$(ck_j/k)(1 - E_{gr} - 2E) < \partial\omega/\partial k_j < (ck_j/k)(1 + E_{gr} + 2E) \qquad j = 1, 2, 3. \tag{9}$$

The errors in numerical reflection and transmission at an interface are controlled by the errors in numerical wave velocity and direction in the media separated by the interface. It can therefore be argued that (4a) and (8a) set bounds also to the errors in reflection and transmission.

The expressions derived here are general, they are easily evaluated numerically, and they considerably simplify the error analysis. Earlier approaches have mainly been carried out as analytical calculations by hand and have been restricted to specific numerical schemes. Note that although the dispersion errors are related to the group velocity, numerical schemes for seismic migration have been, almost exclusively, analysed by examination of the phase errors only.

Result (8) is confirmed by numerical simulations. Figure 2a shows two snapshots of the wavefield resulting from a point source in a 2-D homogeneous acoustic medium. A spatial differentiator with a corresponding maximum relative error in group velocity of 1% was used in the computations and the wavelets are not significantly dispersed. Figure 2b is similar to Fig. 2a but with a maximum relative error in group velocity of 10%. On the first snapshot the wavelet is clearly dispersed and on the second snapshot it is more or less dissolved. A careful examination of the synthesized wavefields verified that the results agree with the theoretical predictions.

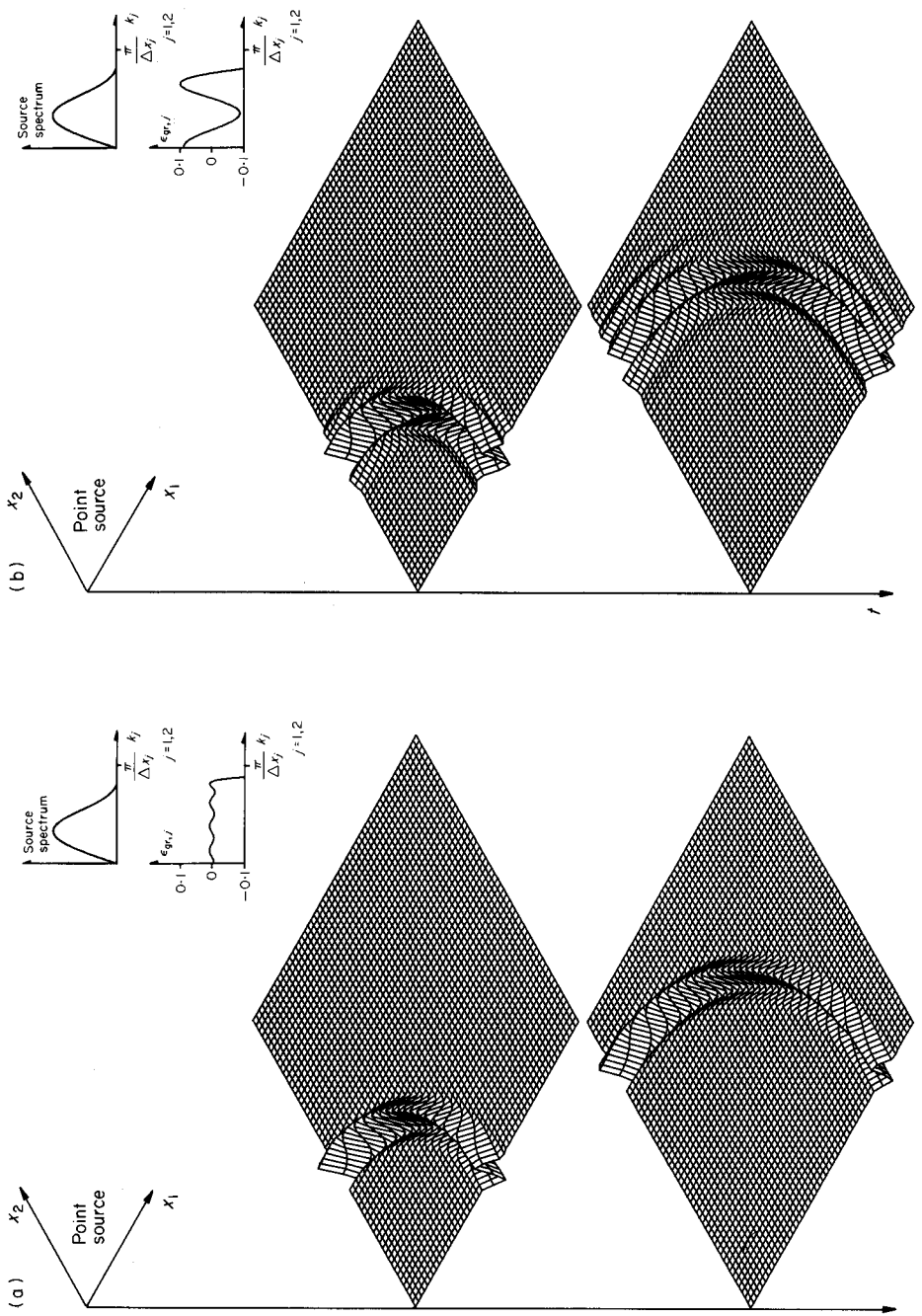

Fig. 2. (a) and (b) Snapshots of the wavefield resulting from a point source in a 2-D homogeneous acoustic medium. The spatial source spectrum and the relative error in group velocity induced by the spatial differentiators are indicated in the upper right corners.

When energy propagates in inhomogeneous media, the spatial frequency spectra of the wavelets are changed according to the local velocity variations. In the next section we demonstrate that, for optimum differentiators, the corresponding relative error in group velocity is an oscillating function of the wavenumber. Consequently, the dispersion errors will not generally accumulate at the maximum possible rate. The homogeneous case treated above may therefore serve as a worst case analysis for inhomogeneous media.

Operators for Numerical Differentiation

Differentiation operators with recursive terms generally give better approximation to the desired amplitude spectrum than pure convolutional (FIR) operators for a given number of arithmetic operations. However, such differentiators do have significant non-linear phase errors (Rabiner and Steiglitz 1970) and are, therefore, not considered here. An FIR approximation is required to obtain a differentiator with no phase distortion (Gibbs 1969). The frequency response of a differentiator is purely imaginary. From the symmetry properties of the Fourier transform it then follows that any FIR approximation to the first derivative must be an antisymmetric operator. The approximate first derivative of a function $u(x_j)$ can thus be written

$$d_{x_j}^{+}(u) = (1/\Delta x_j) \sum_{l=1}^{L} \alpha_l [u(x_j + l\,\Delta x_j) - u(x_j - (l-1)\,\Delta x_j)] \approx \partial/\partial x_j (u(x_j + \Delta x_j/2)), \tag{10a}$$

or

$$d_{x_j}^{-}(u) = (1/\Delta x_j) \sum_{l=1}^{L} \alpha_l [u(x_j + (l-1)\,\Delta x_j) - u(x_j - l\,\Delta x_j)] \approx \partial/\partial x_j (u(x_j - \Delta x_j/2)), \tag{10b}$$

where α_l, $l = 1, 2, \ldots, L$ are coefficients to be chosen optimally in some sense. $2L$ is the length of the operator.

The half-sample shift in (10) is introduced because this step makes the approximation problem for the first derivative easier and yields significantly improved accuracy for a given operator length (Rabiner and Schafer 1974). The operator (10) evaluates the derivative midway between grid points. One should therefore be prepared to use interpolation operators to evaluate parameter and/or function values at such locations. The application of (10) to approximate spatial derivative terms in acoustic and elastic wave calculations for heterogeneous media is discussed in appendix B.

Conventional finite-difference differentiators

The classical FD differentiators are constructed by choosing the coefficients α_l, $l = 1, 2, \ldots, L$ so that the most significant error terms in the Taylor expansion of (10) are cancelled. $2L$ is then the order of the approximation.

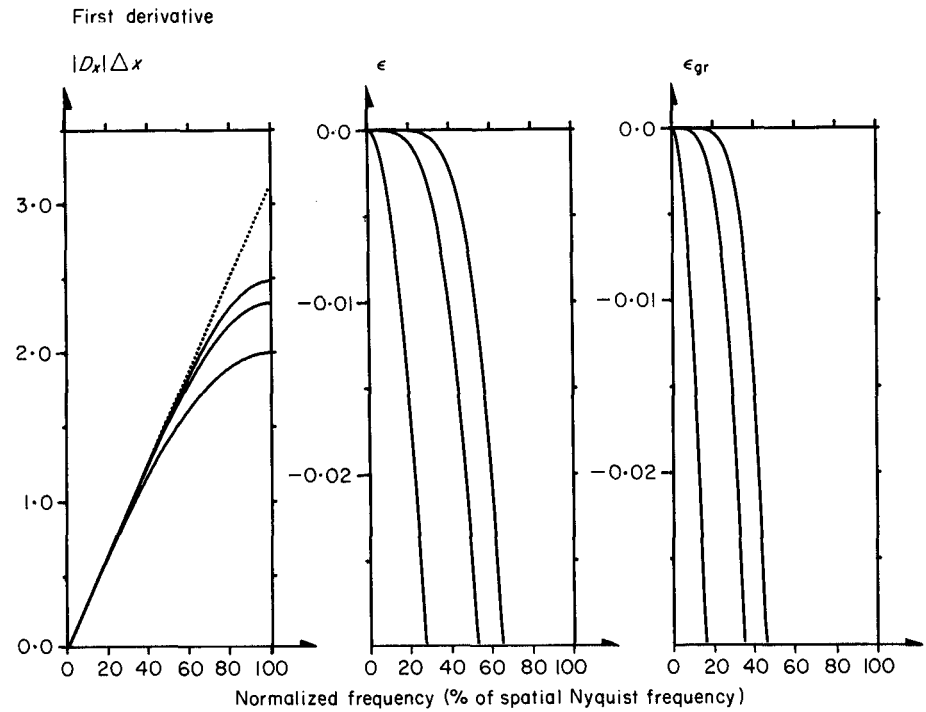

Fig. 3. Frequency responses for conventional FD approximations to the first derivative of second, fourth and sixth order together with their relative error in frequency response and their corresponding relative error in group velocity.

In fig. 3 the frequency responses of the FD approximations to the first derivative of second, fourth and sixth order are displayed together with their relative error in frequency response and their corresponding relative error in group velocity given by (7). The FD design method produces differentiators that become infinitely accurate as the frequency approaches zero, but progressively inaccurate as the Nyquist frequency is approached. In conventional numerical simulation we try to avoid unacceptable dispersion by choosing a small sampling interval relative to the shortest wavelength present. This corresponds to using a high spatial Nyquist frequency relative to the highest spatial frequency of the solution. Thus the energy of the solution is kept within the most accurate part of the frequency response of the differentiator.

Optimum differentiators

Although the conventional FD technique has been regarded practically as a definition of numerical differentiation, the basic design principle for the construction of ordinary FD operators has been created without physical insight. Rather than minimizing the error measured in terms of higher order derivatives, one should minimize

the undesirable effects on the resulting numerical simulations. For wave equation computations it is then natural to optimize the differentiators by minimizing the relative error in the components of the group velocity vector. From (5), this approach would lead to a multi-dimensional error function which is not desirable from a practical point of view.

From the above analysis, i.e., (8) and (9), however, it should be clear that the absolute and directional group velocity errors can be controlled, and to a good approximation even minimized, by minimizing the 1-D expressions for ε_j and $\varepsilon_{gr,\,j}$, $j = 1, 2, 3$. One finds that the phase errors are generally much smaller than the group errors. A small $\varepsilon_{gr,\,j}$ seems to guarantee an even smaller ε_j. It therefore suffices to optimize the differentiators by minimizing the peak relative error in group velocity; i.e., by minimizing

$$\varepsilon_{gr} = \max_{0 \le k_j \le K_c} [k_j \, \partial\varepsilon_j/\partial k_j + \varepsilon_j] \tag{11a}$$

with

$$\varepsilon_j = (D_{x_j}(k_j) e^{\pm i k_j \Delta x_j/2} - i k_j)/i k_j, \tag{11b}$$

where K_c is the spatial bandwidth of the differentiator and $D_{x_j}(k_j)$ is the spatial frequency response of (10). The linear phase term $e^{\pm i k_j \Delta x_j/2}$ is introduced to correct for the half-sample positive or negative delay in (10).

Equiripple filter design is now a standard technique in digital signal processing (McClellan, Parks and Rabiner 1976). However, because of the unconventional error criterion (11a), commercially available software packages for optimum filter design are not directly applicable. A less pedantic approach, which performs adequately for reasonable operator lengths, is to minimize

$$J = \int_{k_j=0}^{K_c} (k_j \, \partial\varepsilon_j/\partial k_j + \varepsilon_j)^4 \, dk_j. \tag{12}$$

This is a least-squares problem which can be solved by standard numerical techniques (Wolfe 1978; Moore, Garbow and Hillstrøm 1980).

For numerical simulation, a more interesting problem is: for a specified accuracy requirement, to design the differentiator that has the largest possible bandwidth for a given operator length; i.e., maximize K_c with the constraint that $\varepsilon_{gr} \le E_{gr}$, where ε_{gr} is given by (11) and where E_{gr} is the specified minimum accuracy. This approach guarantees that no energy within the spatial bandwidth of the differentiator will propagate with a relative error in velocity larger than E_{gr}. The design problem can then be formulated: for a given operator length, solve (12) for increasing values of K_c until the highest K_c is reached that produces a differentiator to satisfy the specified accuracy requirement. For levels of maximum relative error in group velocity ranging from 0.03% to 3%, such differentiators have been designed for operator lengths between 2 and 30 samples.

An example of the behaviour of these differentiators for $E_{gr} = 0.3\%$ is shown in fig. 4 where the frequency responses of the differentiators, their relative error in frequency response and their corresponding relative error in group velocity are

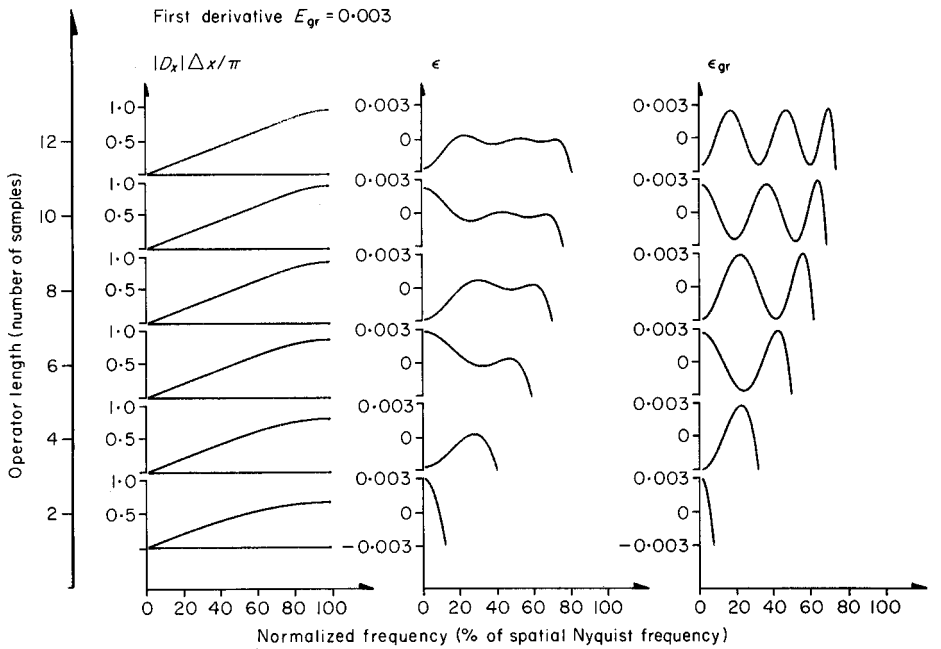

Fig. 4. Frequency responses for optimum differentiators with maximum relative error in group velocity equal to 0.3% together with their relative error in frequency response and their corresponding relative error in group velocity.

plotted for different operator lengths. Note that because the errors are now allowed to oscillate within certain limits, the bandwidths of the optimized differentiators are increased significantly relative to the bandwidths of the conventional differentiators in fig. 3. Also the errors in phase velocity are generally much smaller than the errors in group velocity. Similarly, if the differentiators are optimized by minimizing the phase errors only, the group errors may display peaks up to one order of magnitude larger than the maximum phase errors within the frequency band considered in the optimization.

The properties of the designed differentiators are summarized in fig. 5 which gives the relation between operator length and required number of grid points per wavelength with the maximum relative error in group velocity as a parameter. The number of grid points per wavelength required to attain a specified accuracy is seen to decrease rapidly to a 'reasonable' level of about 2.5 and thereafter approach 2.0 points per wavelength asymptotically.

Note that the relative error is left unconstrained for $k_j > K_c$. This is adequate for applications formulated as time evolution problems, i.e., time evolution modelling and reverse time migration. However, for applications where the wavefield is recursively extrapolated in depth or any other spatial direction, the operators must be more carefully designed to prevent evanescent energy from growing exponentially. Note also that in computations involving one-way wave equations there are

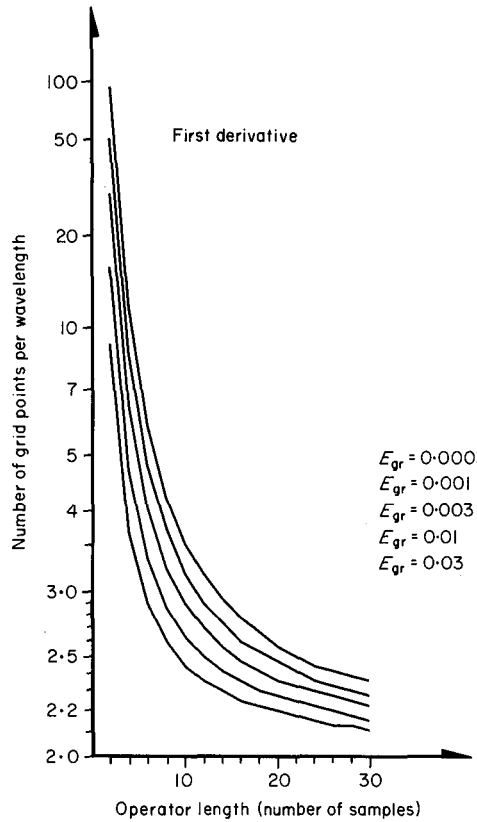

Fig. 5. The relation between operator length and required sampling interval for different levels of maximum relative error in group velocity.

two sources of error: numerical differentiation and series expansion of the wave propagator. Extrapolation operators for one-way wave equations should be optimized by simultaneously taking both sources of error into account to minimize the numerically induced dispersion.

Computational Aspects

The relation between algorithm and computer architecture is not trivial. On parallel computers, including conventional vector computers, the performance may vary by an order of magnitude depending on the suitability of the algorithm to the architecture of the computer (Hockney 1984; Neves 1984).

No generally accepted method exists to judge the suitability of an algorithm or to perform comparisons between different algorithms. The traditional scalar

operations' count is clearly inadequate as it ignores data movement time and delays due to synchronization (Jordan 1982). Algorithms that are slower, in terms of the number of arithmetic operations, may yield considerably higher computational throughput than algorithms designed to minimize the number of arithmetic operations.

A good algorithm balances I/O and memory needs with the speed of the arithmetic unit(s). Therefore, accurate comparisons of the computational efficiency of different numerical schemes generally cannot be made without a detailed analysis of the hardware configuration on which the algorithms are to run. However, for algorithms that have identical overall structures, it seems reasonable to compare the numbers of arithmetic operations, memory operations and I/O operations required by each computational step. The relation between operator length and the required number of grid points per wavelength, for a required accuracy, provides a suitable starting point for such comparisons.

Generally, for explicit 3-D numerical schemes that differ only in the length of the differentiation operator (and the corresponding spatial sampling rate), the number of I/O operations increases as a cubic function of the spatial sampling rate. Similarly, the number of memory operations is cubic in the spatial sampling rate but, at most, linear in the operator length. The number of arithmetic operations is also cubic in the spatial sampling rate and algorithms can be formulated for which the number of arithmetic operations is only linear in the operator length. From fig. 5 it is then easy to infer that the choice of operator for numerical differentiation will have significant impact on the computational efficiency of the resulting scheme.

The simple implementations of FD schemes use regular grid systems which must be scaled according to the size of the problem and the shortest wavelength present. More sophisticated implementations attempt performance improvement by adapting the grid to put a fine mesh wherever short wavelengths occur. Such procedures generally lead to irregular and complicated numerical codes. A much simpler approach, which becomes natural when the sampling interval is no longer the only degree of freedom, is to use a fixed homogeneous mesh and then to select the local differentiator bandwidth according to the local shortest wavelength. Such a procedure can easily be implemented by addressing the operator weights in (10) with the spatial velocity function. This possibility is yet to be investigated in depth.

The spatial grid system represents a 3-D rectangular plug of the real earth. To make the waves propagate through the boundaries of the model rather than to be reflected, proper boundary conditions must be introduced. Absorbing boundary conditions for wave equation computations is still an area of active research. No generally satisfactory solution to this problem has been published so far. A simple intuitive approach is to surround the data volume with a dissipative buffer zone in which the amplitudes are gradually attenuated. Such procedures perform adequately when the width of the buffer zone is about ten shortest wavelengths (Cerjan, Kosloff, D., Kosloff, R. and Reshef 1985). With a spatial sampling rate of more than 20 grid points per shortest wavelength, this method is unwieldy. However, with a spatial sampling rate of 2.5 points or less per wavelength, the method becomes attractive.

APPLICATION EXAMPLE: MODELLING OF ACOUSTIC WAVES IN INHOMOGENEOUS MEDIA

This example is easy to analyse and addresses most of the issues found in more complex situations.

The evolution of acoustic waves in 3-D inhomogeneous media is governed by the scalar wave equation

$$(1/\rho c^2)\,\partial^2 P/\partial t^2 = \sum_{j=1}^{3} \partial/\partial x_j(\rho^{-1}(\partial P/\partial x_j)) + s, \tag{13}$$

where P denotes pressure, ρ is the density and s is a source term. When the spatial derivative terms are computed as explained in appendix B, and a conventional second order FD operator is used for time differentiation, an explicit formulation for the direct numerical solution of (13) is

$$P_{n+1} = 2P_n - P_{n-1} + \kappa[\mathrm{d}_x(\rho^{-1}\,\mathrm{d}_x(P_n)) + \mathrm{d}_y(\rho^{-1}\,\mathrm{d}_y(P_n)) + \mathrm{d}_z(\rho^{-1}\,\mathrm{d}_z(P_n))], \tag{14}$$

with

$$\kappa = \rho c^2(\Delta t)^2,$$

where $x = x_1$, $y = x_2$, $z = x_3$ and where the $\pm$ indices on the differentiation operators defined in (10) have been dropped for convenience. P_n denotes pressure at time $t = n\,\Delta t$. It is assumed that a separate start-up procedure has accounted for the initial conditions and has computed the spatial pressure distribution at two subsequent time steps. By formulating (13) as a set of two coupled first-order equations which can be integrated in time by any stable and accurate numerical technique, the total number of time steps can be reduced. However, to keep the analysis simple, we shall use (14).

The von Neumann stability condition for (14) is given in appendix C. To keep the error in time differentiation comparable to or smaller than the error in spatial differentiation, a small temporal sampling interval Δt must be used. The stability condition (C5) will therefore not be violated in any realistic application. A general stability analysis for inhomogeneous media was not performed. Numerous experiments, however, indicate that (C5) ensures stability even for highly inhomogeneous media.

An example of the application of a 2-D implementation of (14) is shown in figs 6 and 7. This example considers acoustic wave propagation in a region consisting of two materials with different velocities and densities separated by a 90° corner (fig. 6a). The source wavelet had a high-cut frequency of 25 Hz to produce a shortest wavelength of 60 m in the low velocity region. The computations used spatial and temporal grid spacings of 25 m and 2 m respectively, corresponding to 2.4 grid points per shortest wavelength in space and 20 grid points per shortest wavelength in time. An operator with a corresponding peak relative error in group velocity of 1% was used for spatial differentiation. The resulting time histories of the pressure,

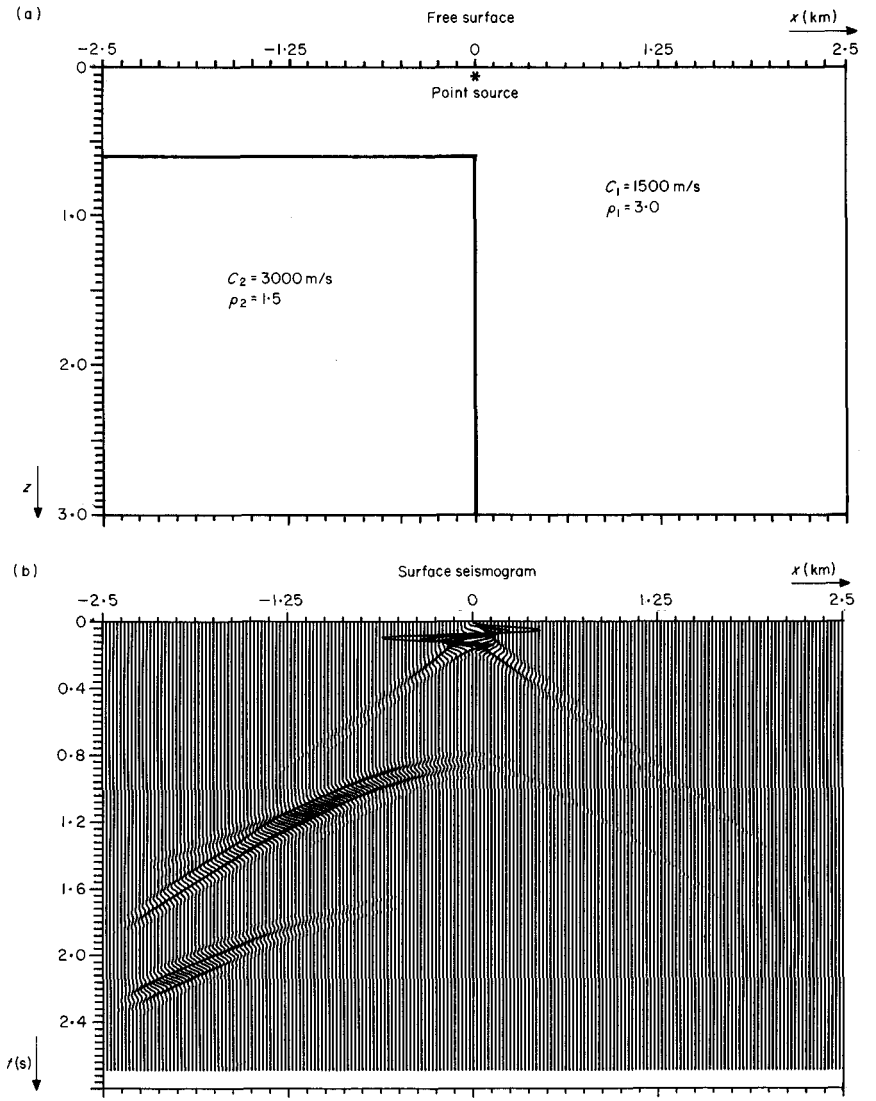

Fig. 6. (a) 90° corner model for acoustic wave propagation. (b) Synthetic surface seismogram for the model in fig. 6a.

recorded 25 m below the free surface, are displayed without scaling in fig. 6b. This synthetic section is easily interpreted by examination of the snapshots of the spatial pressure distribution displayed in fig. 7. The first event to reach the surface is the reflection from the horizontal interface and the head wave connecting the reflected and the transmitted waves. The diffraction from the corner can also be seen. The last visible event on this display is the first multiple of the reflection at the horizontal interface.

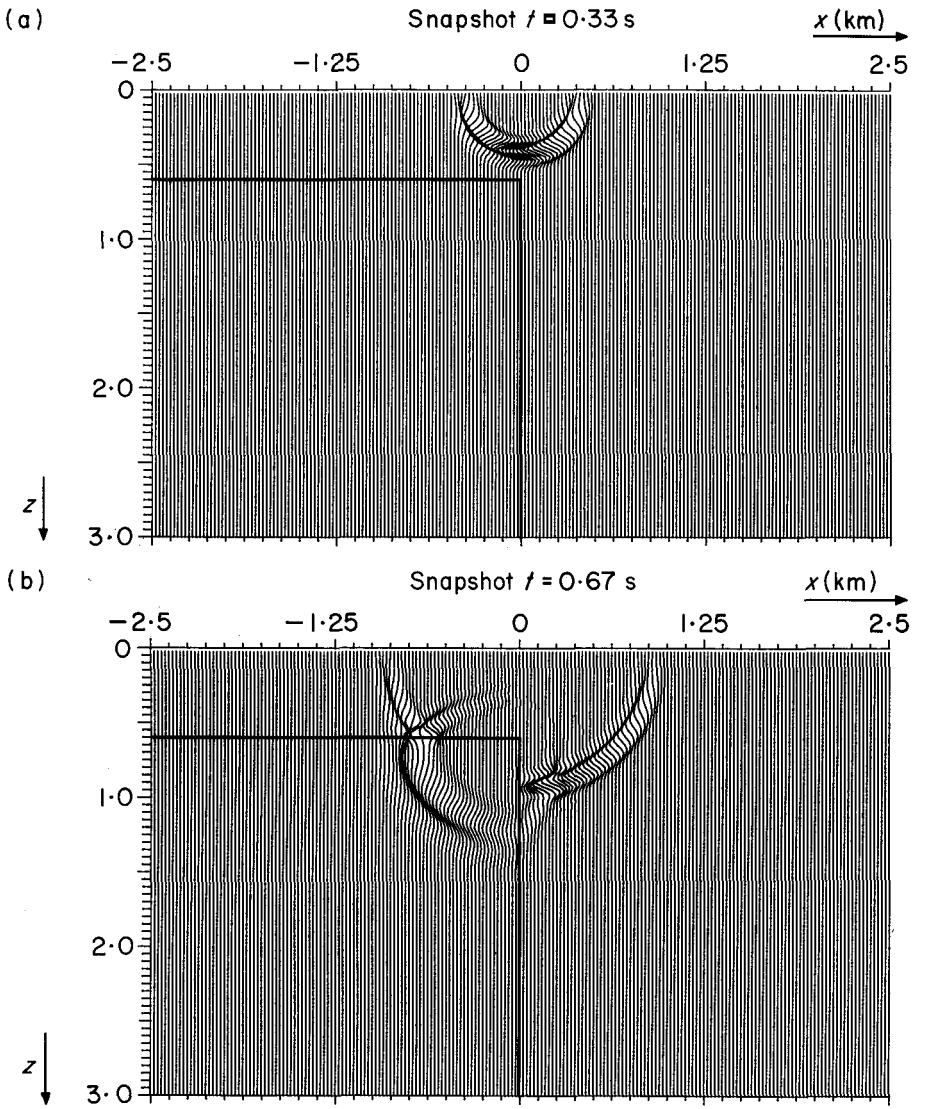

Fig. 7. Snapshots of the spatial pressure distribution for the model in fig. 6a.

The rest of this section is devoted to the analysis of three alternative schemes to compute the right-hand side of (14) as a function of $2L$, the length of the differentiation operators. The level of maximum relative error in group velocity is fixed at 0.3% which is reasonable for the modelling of realistic seismic phenomena. For comparisons we employ a hypothetical data volume whose dimensions are measured by the number of shortest wavelengths and for which the spatial sampling rate is 2.0 grid points per shortest wavelength. All figures concerning the number of

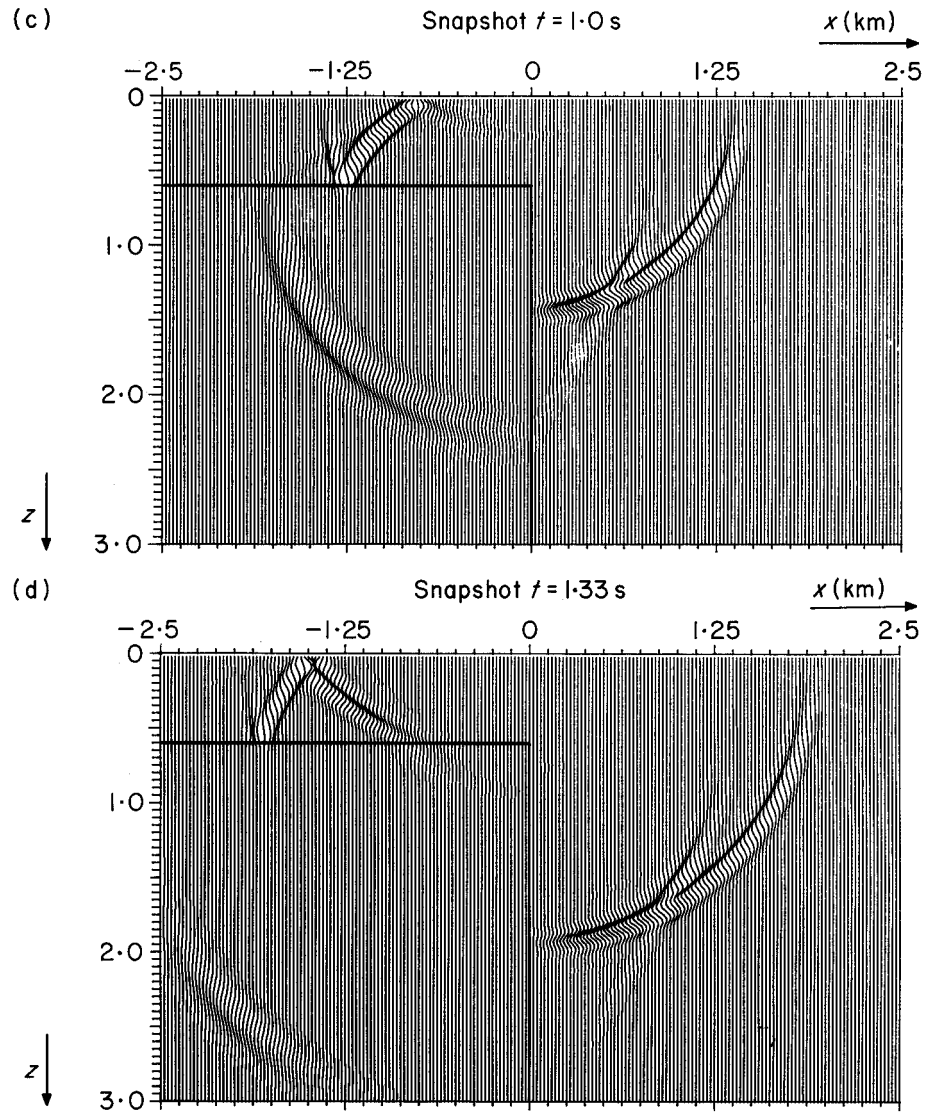

Fig. 7. cont. Snapshots of the spatial pressure distribution for the model in fig. 6a.

computer operations are normalized to represent the number of operations per time step per grid point for the hypothetical data volume.

In this order of magnitude analysis, one add–multiply–add operation counted as one arithmetic operation. This is relevant for convolution with symmetric operators of the type (10) and also for Fast Fourier Transforms (Brigham 1974). However, because twice as many additions as multiplications are to be executed, these problems will be add-bound on vector architectures with only one add-pipeline for every

multiply-pipeline. For such architectures the arithmetic operations count given in the figures below should be doubled to give the equivalent number of multiply–add operations.

It is assumed that the data can be transferred to and from the mass storage system in large blocks so that the associated overhead can be neglected. The number of I/O operations given below represent the number of data words to be transferred sequentially.

The spatial density and velocity functions are assumed to be known at all points in the computational domain. These functions are often treated as piecewise constant functions which change values only at the boundaries of the subsurface layers. The problem to describe general 3-D geometries is a serious concern. To avoid an involved discussion we assume that the density and velocity for each grid point is stored on mass storage or that these parameters can be supplied by a subsystem at a rate no lower than the sequential transfer rate of the mass storage system.

Molecular scheme

Conventional FD schemes have often been implemented by combining all terms on the right-hand side of (14), to yield a so-called computational molecule which is used to step the solution forward in time. To compute P_{n+1} from P_n and P_{n-1} the computational molecule is first applied to all x-vectors $P_n(x, y_j, z_k)$ within the plane $z = z_k$. This process is then repeated for all values of z. During the computation of the new pressure values in the plane $z = z_k$, data within a superplane of 'thickness' $4L - 1$ should be kept in the random access memory of the computer. This memory requirement may be reduced by using a pencil data structure rather than the superplane.

In fig. 8a the molecular scheme is given in quasi-code. The corresponding normalized number of arithmetic, memory and I/O operations is plotted as a function of the length of the differentiation operators in fig. 8b. The number of arithmetic, memory and I/O operations may be reduced respectively by more than $1\frac{1}{2}$, 2, and $2\frac{1}{2}$ orders of magnitude by increasing the operator length from two to eight samples. Thereafter, I/O can be traded for arithmetic operations. In this scheme the absolute number of arithmetic operations increases as L^2 because the terms $\rho^{-1}\, \mathrm{d}_{x_j}(P_n)$ are computed $2L$ times for each grid point for each time step. To overcome this problem the following scheme is proposed.

Quasi-convolutional scheme

The right-hand side of (14) is now computed for each plane $z = z_k$ in three separate passes. In the pass for the z-derivatives, $\rho^{-1}\, \mathrm{d}_z(P_n)$ is first computed for the first x-vector $P_n(x, y_1, z_{k+L})$ in the plane $z = z_{k+L}$. Then $\mathrm{d}_z(\rho^{-1}\, \mathrm{d}_z(P_n))$ is computed for the first x-vector in the plane $z = z_k$. This process is repeated for all y-coordinates. In the pass for the y-derivatives, $\rho^{-1}\, \mathrm{d}_y(P_n)$ is first computed for the first y-vector $P_n(x_1, y, z_k)$ in the plane $z = z_k$. Then $\mathrm{d}_y(\rho^{-1}\, \mathrm{d}_y(P_n))$ is computed for the same vector. This process is repeated for all x-coordinates. The x-derivatives are computed in a pass similar to the pass for the y-derivatives.

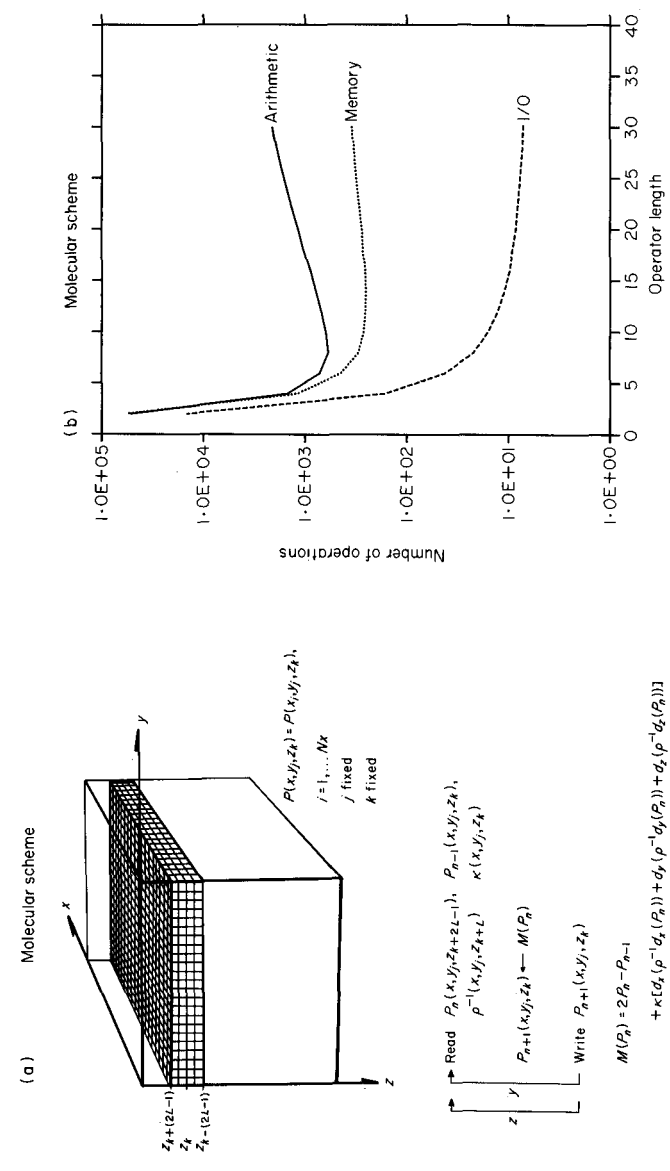

Fig. 8. (a) Quasi-code for the molecular scheme. (b) Normalized number of computer operations for the molecular scheme as functions of the length of the differentiation operator for maximum relative error in group velocity equal to 0.3%.

The procedure involving the three separate passes described above is repeated for all planes $z = z_k$. During the computation of the new pressure values in the plane $z = z_k$, data within a superplane of 'thickness' $4L - 1$ should be kept in random access memory. Again, the memory requirement may be reduced by using a pencil data structure.

In fig. 9a the quasi-convolutional scheme is given in quasi-code. The corresponding normalized number of arithmetic, memory and I/O operations is plotted as a function of the length of the differentiation operator in fig. 9b. An increase in the operator length from two to fourteen samples produces a decrease in the number of arithmetic and memory operations of roughly $2\frac{1}{2}$ orders of magnitude and a decrease in the number of I/O operations of roughly 3 orders of magnitude. By further increasing the operator length, communication can be traded for computation.

Convolutional scheme

In this scheme the right-hand side of (14) is computed for the complete data volume in three separate passes. In the pass for the x-derivatives, $\rho^{-1}\, \mathrm{d}_x(P_n)$ is first calculated for one x-vector $P_n(x, y_j, z_k)$. Then $\mathrm{d}_x(\rho^{-1}\, \mathrm{d}_x(P_n))$ is computed for the same x-vector. This process is repeated for all y- and z-coordinates. The y- and z-derivatives are computed in similar orthogonal passes.

This convolutional scheme requires that the complete data volume is accessed in orthogonal directions for each computational step. Reasonably efficient database systems for such schemes can be implemented by storing the data as 3-D subsets of the complete data volume (Johnson 1984). However, in this application the use of sequential mass storage units is generally unattractive. The memory requirement for efficient utilization of such schemes in the modelling of realistic seismic phenomena is about one gigabyte, provided that the spatial sampling rate does not significantly exceed two points per shortest wavelength. Few computers, at present, are installed with such large random access memories. However, with state-of-the-art (1985) technology, central memories of one gigabyte or more are feasible and such systems should be available commercially in the near future.

In fig. 10a the convolutional scheme is given in quasi-code. The corresponding normalized number of arithmetic and memory operations is given as a function of the operator length in fig. 10b. Because of the memory requirements, application of the shortest operators is impossible. The minimum number of arithmetic operations is reached for an operator length of roughly fourteen samples. Thereafter, the memory requirement may be further reduced at the cost of extra computation.

Note that this scheme is equivalent to the schemes described by Kosloff and Baysal (1982), the difference being that the spatial differentiation is now performed by linear convolution rather than by Fourier-transformation followed by multiplication and back transformation. For comparison with the Fourier method we now assume that our hypothetical data volume measures 128 shortest wavelengths in each of the spatial dimensions. The resulting normalized number of arithmetic and memory operations is indicated by circles in fig. 10b. For this example, the Fourier

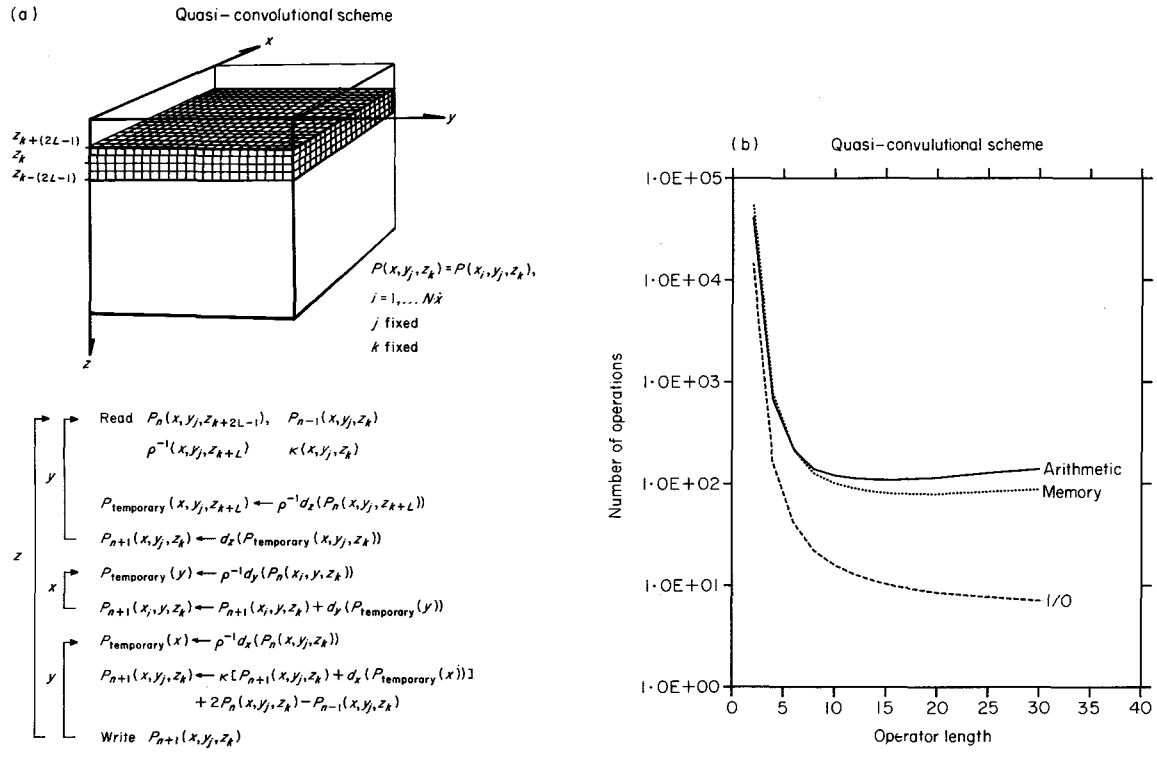

Fig. 9. (a) Quasi-code for the quasi-convolutional scheme. (b) Normalized number of computer operations for the quasi-convolutional scheme as functions of the length of the differentiation operator for maximum relative error in group velocity equal to 0.3%.

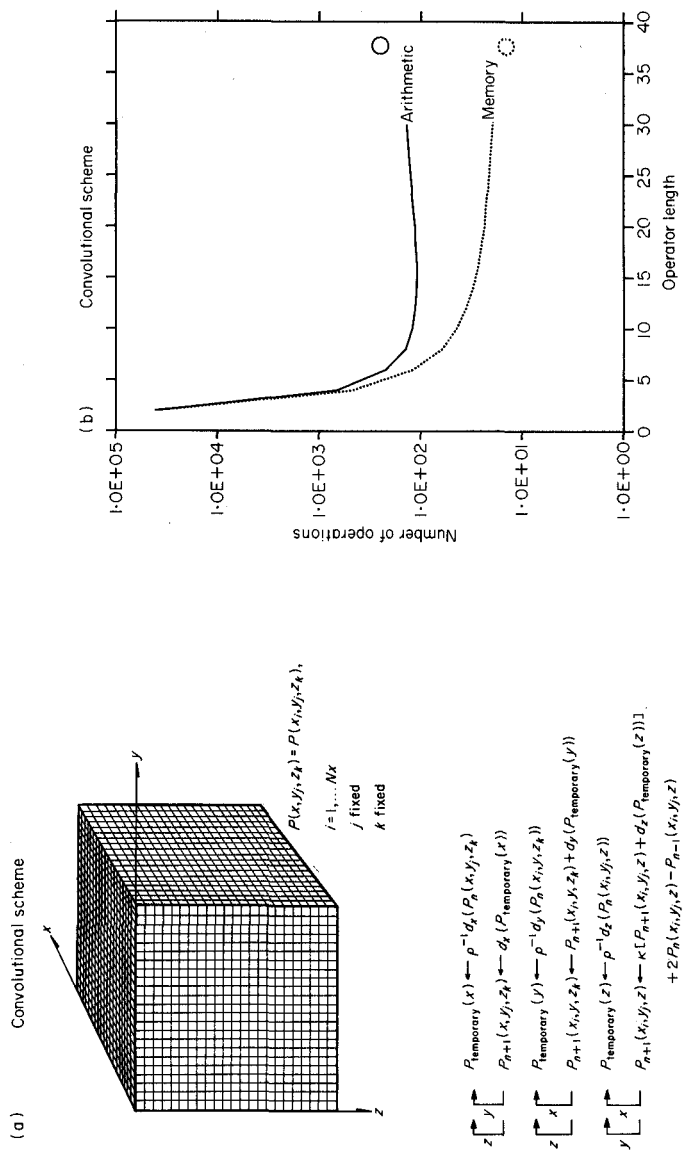

Fig. 10. (a) Quasi-code for the convolutional scheme. (b) Normalized number of computer operations for the convolutional scheme as functions of the length of the differentiation operator for maximum relative error in group velocity equal to 0.3%.

method requires approximately twice as many arithmetic operations as the convolutional scheme. By treating two real sequences as one complex sequence in the Fast Fourier Transforms a factor of two can be gained in computational efficiency (Brigham 1974, Swarztrauber 1982), and then the Fourier method becomes comparable to the convolutional scheme with respect to the arithmetic workload. Both methods are easy to vectorize.

Conclusions

A general high-order finite-difference method for spatial differentiation in wave equation computations has been developed. Within this framework the dispersion analysis is simplified considerably. This new approach offers a substantial reduction in the number of grid points at the cost of a comparatively small increase in the number of arithmetic operations per grid point. This advantage intensifies as the size of the problem expands relative to the shortest wavelength present. For realistic geophysical problems, algorithms can be implemented that require fewer arithmetic and I/O operations, by orders of magnitude compared to conventional second-order finite difference schemes, to yield results with a specified minimum accuracy.

With respect to the arithmetic workload the generalized difference method is comparable to the Fourier method. However, the new approach offers significant improvements in computational flexibility over the Fourier method and efficient implementation does not rely on massive memory facilities. The local nature of the finite-difference operators makes this a promising method for implementation on truly parallel computers.

Although the design criterion according to which the differentiators should be optimized is likely to depend on the problem, similar procedures to the one outlined may also be of interest in other areas of computational physics or numerical simulation.

Acknowledgements

I wish to thank Bjørn Ursin and Børge Arntsen for valuable discussions. I am also grateful to the reviewers for their constructive comments on the manuscript.

Appendix A

Dispersion Relations for Wave Equation Computations

For a lossless isotropic medium, the elastic wave equations for the displacements can be written as

$$\rho\, \partial^2 u_j/\partial t^2 = \sum_{i=1}^{3} \delta_{ij}\, \partial/\partial x_i \left(\lambda \sum_{l=1}^{3} \partial u_l/\partial x_l \right) + \sum_{i=1}^{3} \partial/\partial x_i (\mu(\partial u_j/\partial x_i + \partial u_i/\partial x_j)),$$

$$j = 1, 2, 3, \qquad \delta_{ij} = 1 \text{ for } i = j,\ 0 \text{ else} \qquad \text{(A1)}$$

where u_j are the components of the displacement vector, ρ is the density, and λ and μ are the Lame parameters of the particular medium. For a homogeneous medium, and when the exact spatial differentiators are substituted with operators given by (1), (A1) can be expressed in the frequency-wavenumber domain as

$$-\rho\omega^2\begin{bmatrix}u_1\\u_2\\u_3\end{bmatrix} = \begin{bmatrix}(\lambda+2\mu)D_{x_1}^2+\mu(D_{x_2}^2+D_{x_3}^2), & (\lambda+\mu)D_{x_1}D_{x_2}, & (\lambda+\mu)D_{x_1}D_{x_3}\\ (\lambda+\mu)D_{x_1}D_{x_2}, & (\lambda+2\mu)D_{x_2}^2+\mu(D_{x_1}^2+D_{x_3}^2), & (\lambda+\mu)D_{x_2}D_{x_3}\\ (\lambda+\mu)D_{x_1}D_{x_3}, & (\lambda+\mu)D_{x_2}D_{x_3}, & (\lambda+2\mu)D_{x_3}^2+\mu(D_{x_1}^2+D_{x_2}^2)\end{bmatrix} \times \begin{bmatrix}u_1\\u_2\\u_3\end{bmatrix}, \quad \text{(A2)}$$

where u_j now represent transformed displacements. An eigenvalue decomposition of (A2) reveals

$$-\rho\omega^2 = (\lambda+2\mu)\sum_{j=1}^{3} D_{x_j}^2 \quad \text{(A3a)}$$

and

$$-\rho\omega^2 = \mu\sum_{j=1}^{3} D_{x_j}^2, \quad \text{(A3b)}$$

corresponding to one compressional mode and two shear modes respectively. The elastic wave equations for the stresses (Kosloff and Baysal 1982) yield identical propagating modes. The acoustic wave equation ($\mu = 0$ in (A1)) gives (A3a) directly.

APPENDIX B

APPROXIMATION OF SPATIAL DERIVATIVE TERMS IN WAVE EQUATION COMPUTATIONS

Both the acoustic and the elastic wave equation (A1) for heterogeneous media contain spatial derivative terms of the type

$$\partial/\partial x_j[\beta\ \partial/\partial x_j(u)], \quad \text{(B1)}$$

to be evaluated at locations that coincide with the spatial grid for u. The parameter β equals ρ^{-1} for the acoustic wave equation and $\lambda + 2\mu$ or μ in the elastic case. The expression (B1) contains partial derivatives with respect to one coordinate only and can be computed by the following approximation:

$$\mathrm{d}_{x_j}^{-}[\beta_{x_j}^{+}\ \mathrm{d}_{x_j}^{+}(u)], \quad \text{(B2a)}$$

with

$$\beta_{x_j}^{+} = [\beta(x_j) + \beta(x_j + \Delta x_j)]/2, \quad \text{(B2b)}$$

to be interpreted as follows: first $\partial/\partial_{x_j}(u)$ is computed by the operator (10a) at locations shifted $\frac{1}{2}$-sample in the x_j direction relative to the u grid. At these locations the partial results are multiplied with the parameter β which is evaluated midway between grid points by linear interpolation. By using the operator (10b) for the last differentiation the final result is brought back to locations that coincide with the u grid. The expression (B2) represents a straightforward high-order generalization of the conventional second-order FD expressions (Kelly et al. 1976). A high-order operator could also be used for the evaluation of parameter values midway between grid points but the linear interpolator (B2b) performs adequately. The approximation (B2b) introduces no error into the numerical solution under the assumption that a linear transition zone adequately describes the behaviour of the parameters at a discontinuity. Gupta (1966) showed that the plane wave reflection coefficients for a transition zone are essentially independent of the functional form of the velocity and density variation within the transition zone.

In elastic wave calculations one also has to consider two types of mixed derivatives:

$$\partial/\partial x_j[\lambda\ \partial/\partial x_i(u_i)], \qquad \begin{matrix} i = 1, 2, 3 \\ j = 1, 2, 3 \\ i \neq j \end{matrix} \tag{B3a}$$

and

$$\partial/\partial x_i[\mu\ \partial/\partial x_j(u_i)], \qquad \begin{matrix} i = 1, 2, 3 \\ j = 1, 2, 3 \\ i \neq j \end{matrix} \tag{B3b}$$

both to be evaluated at locations coinciding with the u_j grid. Direct applications of (10) now produce results at locations shifted $\frac{1}{2}$-sample in both the x_i and the x_j directions relative to the u_i grid. This problem can be solved by using centred difference operators for such terms (Kelly et al. 1976) rather than the forward and backward operators (10), or equivalently by using interpolation operators. Because we now interpolate the numerical solution and not the parameters describing the model, the accuracy of the interpolators should be comparable to that of the differentiators.

One can circumvent the problem by exploiting the structure of the elastic wave equation to design grid systems that compensate for the shifting property of the differentiators (10). Let (x_1, x_2, x_3) constitute a reference coordinate system in which the spatial grid for the elastic parameters is represented. Then let the spatial grids for the components of the displacement vector be represented as follows

$$\begin{aligned} u_1 &= u_1(x_1 + \Delta x_1/2, x_2, x_3), \\ u_2 &= u_2(x_1, x_2 + \Delta x_2/2, x_3), \\ u_3 &= u_3(x_1, x_2, x_3 + \Delta x_3/2). \end{aligned} \tag{B4}$$

This grid system has the property that a $\frac{1}{2}$-sample shift in both the x_i direction and the x_j direction brings one from the u_i grid to the u_j grid for $i, j = 1, 2, 3$. Terms of the type (B3) can now be computed by application of the operators (10) and of 2-D linear interpolators for the evaluation of parameter values midway between grid points in terms of the type (B3b). For example the term

$$\partial/\partial x_1[\mu\ \partial/\partial x_2(u_1)] \tag{B5}$$

to be evaluated at the u_2 grid would be computed by the approximation

$$\mathrm{d}^-_{x_1}[\mu^{+\,+}_{x_1 x_2}\ \mathrm{d}^+_{x_2}(u_1)], \tag{B6a}$$

with

$$\mu^{+\,+}_{x_1 x_2} = [\mu(x_1, x_2, x_3) + \mu(x_1 + \Delta x_1, x_2, x_3) + \mu(x_1, x_2, x_3) + \mu(x_1, x_2 + \Delta x_2, x_3)]/4. \tag{B6b}$$

Appendix C

Stability Condition for the Time Evolution of the Scalar Wave Equation

For a medium with constant density and velocity, (14) can be written

$$\begin{bmatrix} P_{n+1} \\ P_n \end{bmatrix} = \begin{bmatrix} 2 - c^2(\Delta t)^2 k^2 \left[1 + \sum_{j=1}^{3} (k_j/k)^2 \varepsilon_j\right]^2 & -1 \\ 1 & 0 \end{bmatrix} \begin{bmatrix} P_n \\ P_{n-1} \end{bmatrix}, \tag{C1}$$

when terms of higher order in ε are neglected. P now denotes transformed pressure. Following Gazdag (1981) I define

$$\theta = c(\Delta t)k\left[1 + \sum_{j=1}^{3} (k_j/k)^2 \varepsilon_j\right]. \tag{C2}$$

The eigenvalues of the matrix in (C1) are

$$\lambda = 2^{-1}[-\theta^2 + 2 + ((\theta^2 - 2)^2 - 4)^{1/2}]. \tag{C3}$$

From (C3) one concludes that $|\lambda| = 1$ for $\theta \leq 2$, or

$$c\ \Delta t \leq 2/k\left[1 + \sum_{j=1}^{3} (k_j/k)^2 \varepsilon_j\right]. \tag{C4}$$

For $\Delta x_j = \Delta x$, $j = 1, 2, 3$ the highest wavenumber k is $k_{\max} = \pi\sqrt{3}/\Delta x$ and the stability condition can be written

$$c\ \Delta t \leq 2\ \Delta x/\pi\sqrt{3}(1 + E), \tag{C5}$$

when

$$|\varepsilon_j| \leq E, \qquad j = 1, 2, 3. \tag{C6}$$

REFERENCES

ALFORD, R.M., KELLY, K.R. and BOORE, D.M. 1974, Accuracy of finite-difference modeling of the acoustic wave equation, Geophysics 39, 834–842.

BRIGHAM, E.O. 1974, The Fast Fourier Transform, Prentice-Hall, Inc.

CERJAN, C., KOSLOFF, D., KOSLOFF, R. and RESHEF, M. 1985, A non-reflecting boundary condition for discrete acoustic and elastic wave equations, Geophysics 50, 705–708.

DABLAIN, M.A. 1986, The application of high-order differencing to the scalar wave equation, Geophysics 51, 54–66.

GAZDAG, J. 1973, Numerical convective schemes based on accurate computation of space derivatives, Journal of Computational Physics 13, 100–113.

GAZDAG, J. 1981, Modeling of the acoustic wave equation with transform methods, Geophysics 46, 854–859.

GIBBS, A.J. 1969, On the frequency domain responses of causal digital filters, Ph.D. thesis, Department of Electrical Engineering, University of Wisconsin.

GUPTA, R.N. 1966, Reflection of plane elastic waves from transition layers with arbitrary variation of velocity and density, Bulletin of the Seismological Society of America 56, 633–642.

HOCKNEY, R.W. 1984, Performance of parallel computers, *in* Proceedings of the NATO Workshop on High Speed Computations, J. Kowalik (ed.), NATO ASI Series, F-7, Springer-Verlag, Inc.

JOHNSON, O.G. 1984, Three-dimensional wave equation computations on vector computers, Proceedings of the IEEE 18-9219, 90–95.

JORDAN, T.L. 1982, A guide to parallel computation and some Cray-1 experiences, *in* Parallel Computations, G. Rodrigue (ed.), Academic Press, Inc.

KELLY, K.R., WARD, R.W., TREITEL, S. and ALFORD, R.M. 1976, Synthetic seismograms: a finite-difference approach, Geophysics 41, 2–27.

KOSLOFF, D. and BAYSAL, E. 1982, Forward modeling by a Fourier method, Geophysics 47, 1402–1412.

KOSLOFF, D., RESHEF, M. and LOEWENTHAL, D. 1984, Elastic wave calculations by the Fourier method, Bulletin of the Seismological Society of America 74, 875–891.

KREISS, H.O. and OLIGER, J. 1972, Comparison of accurate methods for the integration of hyperbolic equations, Tellus 24, 199–215.

MARFURT, K.J. 1984, Accuracy of finite-difference and finite-element modeling of the scalar and elastic wave equations, Geophysics 49, 533–549.

MCCLELLAN, J.H., PARKS, T.W. and RABINER, L.R. 1973, A computer program for designing optimum FIR linear phase digital filters, IEEE Transactions on Audio and Electroacoustics AU-21, 506–526.

MOORE, J.J., GARBOW, B.S. and HILLSTRØM, K.E. 1980, User guide for *MINPACK*-1, Argonne National Laboratory, ANL-80-74.

NEVES, K.W. 1984, Vectorization of scientific software, *in* Proceedings of the NATO Workshop on High Speed Computations, J. Kowalik (ed.), NATO ASI Series, F-7, Springer-Verlag, Inc.

ORZAG, S.A. 1980, Spectral methods for problems in complex geometries, Journal of Computational Physics 37, 70–92.

RABINER, L.R. and SCHAFER, R.W. 1974, On the behavior of minimax relative error FIR digital differentiators, Bell System Technical Journal 53, 333–346.

RABINER, L.R. and STEIGLITZ, K. 1970, The design of wide-band recursive and nonrecursive digital differentiators, IEEE Transactions on Audio and Electroacoustics AU-18, 204–209.

SWARZTRAUBER, P.N. 1982, Vectorizing the FFTs, *in* Parallel Computations, G. Rodrigue (ed.), Academic Press, Inc.

TREFETHEN, L.N. 1982, Group velocity in finite difference schemes, Society of Industrial and Applied Mathematics Review 24, 113–136.

WOLFE, M.A. 1978, Numerical Methods For Unconstrained Optimization, Van Nostrand Reinhold.